Experimental and Quantum Dynamical Study on an Asymmetric Insertion Reaction: State-to-State Dynamics of $O(^1D) + HD(^1\Sigma_g^+, v' = 0, j' = 0) \rightarrow OH(^2\Pi, v'', N'') + D(^2S)$

Kaijun Yuan, Yuan Cheng, Xianghong Liu, Steven Harich, and Xueming Yang*,†

State Key Laboratory of Molecular Reaction Dynamics, Dalian Institute of Chemical Physics, Dalian, Liaoning 116023, People's Republic of China

Dong Hui Zhang*,‡

Center for Theoretical and Computational Chemistry and State Key Laboratory of Molecular Reaction Dynamics, Dalian Institute of Chemical Physics, Chinese Academy of Sciences, Dalian, Liaoning 116023, People's Republic of China

(Received 3 October 2005; published 16 March 2006)

Quantum-state-resolved differential cross sections of the $O(^1D) + HD \rightarrow OH + D$ reaction at the collision energy of 7.11 kJ/mol has been determined experimentally and theoretically. The results of the time-dependent wave-packet calculations are overall in good agreement with the crossed beam scattering data, providing a benchmark example of an asymmetric insertion reaction at the state-to-state scattering level. The good agreement between experiment and theory suggests that the underlying ground potential energy surface is generally correct and that the nonadiabatic effect involving the electronic excited pathway is apparently small in this system.

DOI: 10.1103/PhysRevLett.96.103202 PACS numbers: 34.10.+x, 34.50.Lf, 34.50.Pi

Even though full quantum theoretical dynamical studies at the state-to-state level on direct reactions of triatomic systems are rather straightforward now, full quantum investigation of triatomic systems with deep potential wells is still extremely difficult. In recent years, full quantum dynamical studies of $O(^1D) + H_2$ [1] and $N(^2D) + H_2$ [2] have become possible using the time-independent method with fully converged quantum-state-resolved differential cross-section calculations. However, more complicated systems are still out of reach, even for the above systems with 1 D-atom substitution. Experimentally, full quantum-state-resolved scattering study for reaction systems with deep wells is also challenging.

The reaction of $O(^1D) + H_2$ plays a significant role in atmospheric [3] and combustion chemistry [4]. Extensive experimental and theoretical studies have been carried out in order to elucidate the dynamics of this reaction (and its isotopic variants), as reviewed recently by Casavecchia [5]. Casavecchia and co-workers investigated this system using the universal crossed beam method [6], and Suits and co-workers studied this reaction using the ion imaging technique [7]. More recently, Liu and co-workers [8] measured the excitation function and the differential cross sections at different collision energies for the $O(^1D) + HD$ reaction. At collision energies above 7.53 kJ/mol, an abstraction mechanism was observed in addition to the insertion mechanism. This abstraction reaction mechanism is likely caused by an excited state reaction pathway. The inferred barrier height from this experiment is about 8.79 kJ/mol lower than the theoretical value (9.62 kJ/mol) on the Dobbyn-Knowles (DK) potential energy surface (PES) [9]. Recently, the $O(^1D) + H_2$ reaction has been investigated at the collision energy of 5.44 kJ/mol with nearly full product quantum-state resolution, providing an excellent case for state-to-state insertion chemistry [10,11]. The $O(^1D) + D_2$ reaction has also been investigated experimentally at two different collision energies [12] Interesting dynamics for the $O(^1D) + HD \rightarrow OD + H$ reaction has also been observed [13].

In this Letter, we report the results of a combined theoretical and experimental study on the elementary $O(^1D) + HD$ reaction at the collision energy of 7.11 kJ/mol, both at the full quantum state-to-state scattering level. Experimentally, the reaction $O(^1D) + HD(^1\Sigma_g^+, v' = 0, j' = 0) \rightarrow OH(^2\Pi, v'', N'') + D(^2S) + 179.91$ kJ/mol was studied by using the H(D)-atom Rydberg "tagging" time-of-flight (TOF) technique with very high translational resolution [14]. The D-atom product is detected through a two-step excitation scheme to highly excited Rydberg states in this technique. The 121.6 nm vacuum ultraviolet (VUV) light used in the first step excitation is generated using a two-photon resonant $(2\omega_1 - \omega_2)$ four wave mixing scheme in a Kr/Ar gas cell [15]. After the first step VUV excitation, the D-atom product is then sequentially excited to a high Rydberg state with $n \approx 50$ with 365-nm light. The neutral Rydberg D atom then flies a certain distance for the TOF measurement and reaches a microchannel plate (MCP) detector with a fine metal grid (grounded) in the front. The signal received by the MCP is then amplified by a fast preamplifier and counted by a multichannel scaler. Two parallel molecular beams (HD and O_2) were generated with similar pulsed valves. The $O(^1D)$ atom beam was produced by photolysis of O_2 with 157-nm laser light from an F_2 laser (Lambda Physik LPX 210I). The $O(^1D)$ beam was then crossed at 90° with the HD molecular beam. The HD molecular beam was generated by expanding the HD sample through a pulsed nozzle, which was cooled to the liquid nitrogen temperature (~78 °K). The velocity of the $O(^1D)$ beam has been measured to be 2050 m/s with a very narrow velocity distribution $(v/\Delta v > 50)$, while the ve-

locity of the liquid nitrogen cooled HD beam is 1384 m/s with a speed ratio ($v/\Delta v$) of about 15. Since HD is expanded under the liquid nitrogen temperature, HD molecules in the beam should all be in the $j = 0$ state.

TOF spectra of the D-atom products were measured at 19 laboratory (LAB) angles (from 117° to −60° at about a 10° interval). The measurement error of the relative intensities is about ±10%. The TOF resolution is less than 1%. Three typical TOF spectra are shown in Fig. 1 corresponding to the reaction products at roughly the forward (−60°), sideway (30°), and backward (117°) scattering directions in the c.m. frame. All the sharp structures in these TOF spectra can be clearly assigned to individual OH rovibrational states with certain peaks from overlapped states. These TOF spectra were converted to the c.m. frame using a standard Jacobian transformation to obtain product kinetic energy (KE) distributions obtained. During the conversion, detection efficiencies of the D-atom product at different LAB angles and different velocities were simulated using the experimental parameters and included in the conversion. The KE distributions obtained experimentally in the LAB frame were simulated perfectly by simply adjusting the relative populations of the rotational-vibrational states of the OH product below the energetic limit for the reaction. Since the energies of all the OH rovibrational states are known accurately, the fitting can be done almost perfectly. From these fittings, relative populations of the OH product at different rovibrational states were determined at 18 LAB angles. The population of most OH product rovibrational states can be determined from the fitting accurately. Quantum-state distributions of the OH product in the c.m. frame ($\Theta_{\text{c.m.}} = 0°$ to 180° at a 10° step) were then be determined by a polynomial fit to the above results, and from these distributions, rovibrational-state-resolved differential cross sections were determined. The angular distributions for the OH product at $v = 0$ to 4 were determined by integrating over all of the rotational state populations for each vibrational level. Figure 2 shows the total product angular distribution in the c.m. frame for this reaction by accumulating populations of all OH vibrational levels at different c.m. angles. The total product angular distribution is obviously more or less forward and backward symmetric. In the fitting, there are errors involved. For those rotational states that are not overlapped or partially overlapped, the fitting errors are very small (less than a few percent). There are, however, a small number of totally overlapped OH states that have larger error bars in the population due to the fitting correlations. During the fitting, we used an assumption that the rotational distribution within a same vibrational manifold should not vary widely within a small range of nearby rotational states. The fitting error bars for those totally overlapped states are estimated to be ±20%. The overall error resulting from fitting should not be significantly larger than the measurement error. Therefore the overall error of the experimental results for the rotational distribution should be about 15%–20%, while the error bars for the vibrational state distribution should be larger than 15%.

Total quantum-state distributions for this reaction can be determined by integrating these distributions over different c.m. angles. The OH rotational state distributions for each vibrational level are shown in Fig. 3(a). The distributions for different vibrational states are actually quite similar in which all distributions peak near their energetic limit (high N), indicating that the majority of the OH products from this reaction are significantly rotationally excited. The average product rotational quantum number $\langle N \rangle$ for different OH vibrational state ($v = 0$, 1, 2, 3, and 4) is 19.3, 15.8, 13.5, 9.6, and 5.6. The average rotational energy $\langle E_r \rangle = 44.7$ kJ/mol, which is about 24% of the total available energy. By integrating the rotational state distributions for each vibrational level, the total OH product vibrational state distribution can be determined experimentally

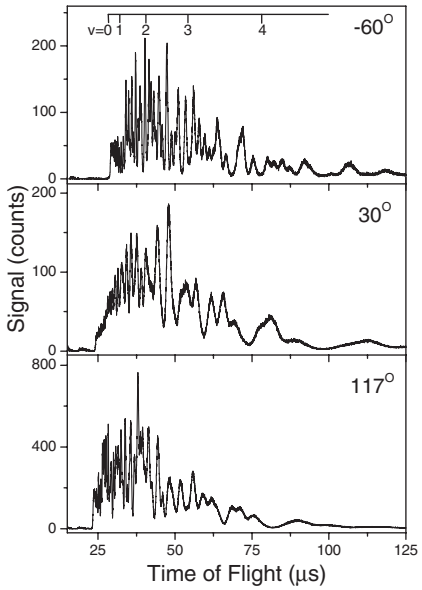

FIG. 1. TOF spectra at three typical laboratory angles (117°, 30°, and −60°) of the D-atom product from the $O(^1D) + HD \rightarrow OH + D$ reaction at the collision energy of 7.11 kJ/mol.

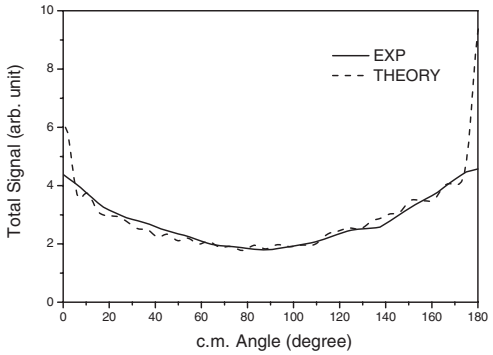

FIG. 2. Experimental and theoretical angular distributions for the total D-atom products from the $O(^1D) + HD \rightarrow OH + D$ reaction at the collision energy of 7.11 kJ/mol.

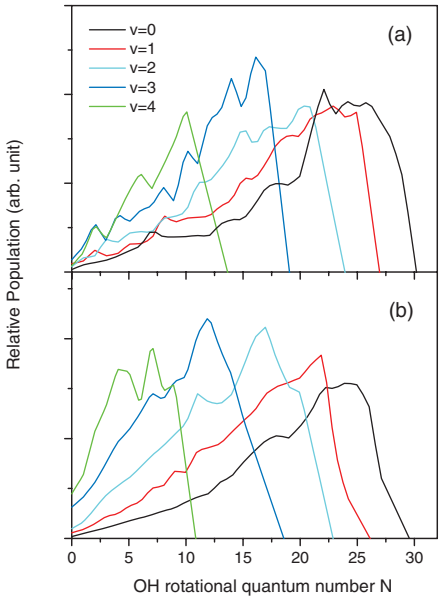

FIG. 3 (color). Rotational distributions of the OH products at different vibrational states for the title reaction at the collision energy of 7.11 kJ/mol. (a) Theoretical results based on full quantum wave-packet calculations on the DK surface; (b) experimental results.

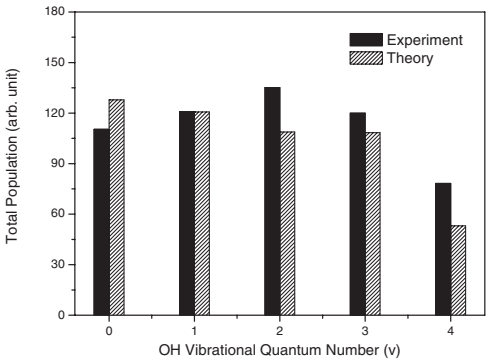

FIG. 4. Vibrational distributions of the OH product from the $O(^1D) + HD \rightarrow OH + D$ reaction at the collision energy of 7.11 kJ/mol. Theoretical results are based on full quantum dynamical calculations on the DK surface.

(Fig. 4). The average product vibrational energy $\langle E_v \rangle = 76.9$ kJ/mol, about 41% of the total available energy. The overall picture of the OH + D channel in the $O(^1D) + HD$ reaction looks similar to the $O(^1D)$ reaction with H_2, such as the OH rotational state distributions and the overall angular distributions. The rotational state-specific angular distributions and the vibrational state distribution are, however, noticeably different for the two reactions. The $O(^1D) + HD$ reaction shows more populations at higher vibrational states than the $O(^1D) + H_2$ reaction [10]. This could partly be due to the asymmetric insertion in the F + HD reaction.

To interpret the above experimental results, fully converged quantum dynamics calculations of state-to-state differential cross sections on the title reaction were carried out using the time-dependent wave-packet methods on the accurate *ab initio* DK PES [9,16]. In the wave-packet calculation, only the ground state reaction is considered. Details of the calculation will be published elsewhere, so only a brief description of the calculation is presented here. An initial wave packet for the $O(^1D) + HD(v = 0, j = 0)$ state was prepared in the reactant Jacobi coordinates, and propagated for 18 000 a.u. from asymptotic region to $R_r = 6.0a_0$ (where R_r is the distance from O atom to the c.m. of HD diatom). It is straightforward to carry out this propagation, because at that R_r distance, only inelastic scattering process between O atom and HD diatom occurs. A coordinate transformation was then carried out to transfer the wave packet from the reactant coordinates to the OH + D product coordinates. After the transformation, we propagated the wave packet for additional 72 000 a.u. in the product coordinates to get converged S-matrix elements. In the product coordinates, we used a total number of 235 sine functions (among them 167 for the interaction region) for the translational coordinate R_p in the range $[0.0, 18]a_0$. A total of 100 vibrational functions are employed in the range $[0.8, 14.0]a_0$ for the product OH. For the rotational basis, we used $j_{\max}^{OH} = 130$, and included all the K components for a total angular momentum J. The final state analysis to obtain S-matrix elements was carried out at $R_p = 13a_0$. The computation is very demanding, considering that this is likely the most difficult insertion reaction system yet been tried for fully converged differential cross-section calculations, demonstrating the powerfulness of the time-dependent wave-packet method used here.

The total product angular distribution from the time-dependent wave-packet calculations is shown in Fig. 2 along with the experimental results. The experimental angular distribution is scaled to the theoretical distribution using a single scaling factor. From Fig. 2, the overall agreement between the theory and experiment is quite good. However, at the forward and backward scattering directions, there are two sharp peaks in the angular distributions that do not agree with experimental results. Similar phenomenon has been reported previously for the $O(^1D) + H_2$ reaction in a full quantum calculation, while these peaks do not appear in the quasiclassical trajectory calculations, implying these sharp peaks are quantum phenomenon. From detailed theoretical analysis, reactive collisions responsible for the forward and backward scattering peaks are nothing special in comparison with collisions responsible for scattering at other angles. This suggests that such high scattering peak is intrinsic for the DK PES. The disagreement between theory and experiment can be traced to different possible sources. First, the experimental angular distribution was measured at an interval of 10° with a 3° detection range and the narrow peaks at the forward and backward directions show only a width of 6°, therefore that these sharp peaks could be partly missed in the experiment. Another possible source of the disagreement is the accu-

racy of the DK PES since the sharp forward/backward scattering peaks are intrinsic for this PES. This disagreement certainly deserves further experimental as well as theoretical investigations. The roughly forward/backward scattering symmetry for the title reaction is quite interesting since the $O(^1D)$ atom is inserting into the asymmetric H-D bond, implying that the overall product forward/backward scattering symmetry in this reaction is resulted from a long-lived complex formation mechanism, and that insertion symmetry is not a significant factor for the product forward/backward symmetry in the $O(^1D)$ insertion reaction with H_2.

Rovibrational state distributions of the OH product from the title reactions were also obtained using the quantum wave-packet method. The theoretical rovibrational state distributions for different OH vibrational states are shown in Fig. 3(a), in direct comparison with the experimental results shown in Fig. 3(b). Even though the theoretical and experimental shapes of the rotational state distribution for each $OH(v)$ are not exactly the same, the overall rotational state distributions do show great similarities. The average theoretical product rotational quantum number $\langle N \rangle$ for different OH vibrational state ($v = 0$, 1, 2, 3, and 4) is 20.5, 17.8, 15.1, 12.0, and 7.9, respectively. The averaged theoretical product rotational energy $\langle E_r \rangle$ is 58.8 kJ/mol, which is about 20% higher than the experimental value (44.7 kJ/mol). It seems that the theoretical calculation overestimate the rotational excitation by a significant amount. This discrepancy could be due partly to the DK PES that might be not accurate enough. Experimental measurement error is also likely a factor. By integrating the rotational state distributions, total OH product vibrational state distribution can also be determined. In Fig. 4, the theoretical OH vibrational state distribution is shown together with the experimentally measured the OH state distribution. The agreement between theory and experiment is quite good considering the experimental measurement error involved. The theoretical averaged vibrational energy is 69.1 kJ/mol, which is slightly less than the experimental value (76.9 kJ/mol). It seems that the theoretical results systematically underestimate the high vibrational state populations. The general agreement between theory and experiment is good. The difference here could partly be due to the neglect of the contribution from the excited state reactions in the present calculations. Since the experiment for this $O(^1D) + HD$ reaction was carried out at 7.11 kJ/mol, which is only slightly below the 7.53 kJ/mol barrier [8], the nonadiabatic excited state pathway might be contributing via quantum tunneling, even though the contribution is likely small.

In this work, we have provided the most detailed experimental and theoretical studies of the $O(^1D)$ insertion reaction with HD using the state-of-art experimental and theoretical methods. The theoretical results are overall in agreement with the experiment observations even though some disagreement remains, suggesting that the reaction proceeds mainly via the ground PES and the nonadiabatic excited state pathway plays a small role at most. This study provides a benchmark example of an asymmetric insertion reaction that can be understood at the full state-to-state scattering level both experimentally and theoretically.

This work is supported by the Chinese Academy of Sciences, the Ministry of Science and Technology, and the National Natural Science Foundation of China.

*To whom correspondence should be addressed.
†Electronic address: xmyang@dicp.ac.cn
‡Electronic address: zhangdh@dicp.ac.cn

[1] F. J. Aoiz, L. Banares, J. F. Castillo, M. Brouard, W. Denzer, C. Vallance, P. Honvault, J.-M. Launay, A. J. Dobbyn, and P. Knowles, Phys. Rev. Lett. **86**, 1729 (2001).
[2] N. Balucani, L. Cartechini, G. Capozza, E. Segoloni, P. Casavecchia, G. G. Volpi, F. J. Aoiz, L. Banares, P. Honvault, and J. M. Launay, Phys. Rev. Lett. **89**, 013201 (2002).
[3] G. Anderson, Annu. Rev. Phys. Chem. **38**, 489 (1987), and references therein.
[4] G. Dixon-Lewis and D. J. Williams, Compr. Chem. Kinet. **17**, 1 (1977).
[5] P. Casavecchia, Rep. Prog. Phys. **63**, 355 (2000).
[6] M. Alagia *et al.*, J. Chem. Phys. **108**, 6698 (1998).
[7] M. Ahmed, D. S. Peterka, and A. G. Suits, Chem. Phys. Lett. **301**, 372 (1999).
[8] D.-C. Che and K. Liu, J. Chem. Phys. **103**, 5164 (1995); Y.-T. Hsu and K. Liu, *ibid.* **107**, 1664 (1997); Y.-T. Hsu, J. H. Wang, and K. Liu, *ibid.* **107**, 2351 (1997); Y.-T. Hsu, K. Liu, L. A. Pederson, and G. C. Schatz, *ibid.* **111**, 7921 (1999); Y.-T. Hsu, K. Liu, L. A. Pederson, and G. C. Schatz, *ibid.* **111**, 7931 (1999).
[9] A. J. Dobbyn and P. J. Knowles, Faraday Discuss. **110**, 247 (1998).
[10] X. Liu, J. J. Lin, S. A. Harich, G. C. Schatz, and X. Yang, Science **289**, 1536 (2000).
[11] F. J. Aoiz, L. Banares, J. F. Castillo, V. J. Herrero, B. Martinez-Haya, P. Honvault, J. M. launay, X. Liu, J. J. Lin, S. A. Harich, C. C. Wang, and X. Yang, J. Chem. Phys. **116**, 10 692 (2002).
[12] X. Liu, J. J. Lin, S. A. Harich, and X. Yang, Phys. Rev. Lett. **86**, 408 (2001).
[13] X. Liu, J. J. Lin, S. Harich, and X. Yang, J. Chem. Phys. **113**, 1325 (2000).
[14] L. Schnieder *et al.*, J. Chem. Phys. **92**, 7027 (1990); Science **269**, 207 (1995); L. Schnieder, K. Seekamp-Rahn, E. Wrede, and K. H. Welge, J. Chem. Phys. **107**, 6175 (1997).
[15] J. P. Marangos, N. Shen, H. Ma, M. H. R. Hutchinson, and J. P. Connerade, J. Opt. Soc. Am. B **7**, 1254 (1990).
[16] G. C. Schatz, L. A. Pederson, and P. J. Kuntz, Faraday Discuss. **108**, 357 (1997); S. K. Gray, C. Petrongolo, K. Drukker, and G. C. Schatz, J. Phys. Chem. A **103**, 9448 (1999); K. Drukker and G. C. Schatz, J. Chem. Phys. **111**, 2451 (1999).